

The $M - \sigma$ relation in different environments

K. Zubovas¹, A.R. King¹

¹*Theoretical Astrophysics Group, University of Leicester, Leicester LE1 7RH*

8 November 2018

ABSTRACT

Galaxies become red and dead when the central supermassive black hole (SMBH) becomes massive enough to drive an outflow beyond the virial radius of the halo. We show that this final SMBH mass is larger than the final SMBH mass in the bulge of a spiral galaxy by up to an order of magnitude. The $M - \sigma$ relations in the two galaxy types are almost parallel ($M \propto \sigma^{4+\beta}$, with $\beta < 1$) but offset in normalization, with the extra SMBH mass supplied by the major merger transforming the galaxy into an elliptical, or by mass gain in a galaxy cluster. This agrees with recent findings that SMBH in two Brightest Cluster Galaxies are $\sim 10\times$ the expected $M - \sigma$ mass. We show that these results do not strongly depend on the assumed profile of the dark matter halo, so analytic estimates found for an isothermal potential are approximately valid in all realistic cases.

Our results imply that there are in practice actually *three* $M - \sigma$ relations, corresponding to spiral galaxies with evolved bulges, field elliptical galaxies and cluster centre elliptical galaxies. A fourth relation, corresponding to cluster spiral galaxies, is also possible, but such galaxies are expected to be rare. All these relations have the form $M_{\text{BH}} = C_n \sigma^4$, with only slight difference in slope between field and cluster galaxies, but with slightly different coefficients C_n . Conflating data from galaxies of different types and fitting a single relation to them tends to produce a higher power of σ .

Key words: galaxies:evolution - quasars:general - black hole physics - accretion

1 INTRODUCTION

In the past decade, observations of large numbers of galaxies have revealed important correlations between the properties of galaxy spheroids and the supermassive black holes (SMBHs) they host. Two of these relations are particularly interesting: the black hole mass – host spheroid velocity dispersion ($M - \sigma$) relation (Ferrarese et al. 2006) and the black hole - bulge mass ($M - M_b$) relation (Häring & Rix 2004). Together, they strongly imply that SMBHs coevolve with their hosts, and probably affect each other’s evolution through some form of feedback.

There have been numerous attempts to explain these relations, both analytically (Silk & Rees 1998; King 2003, 2005; Murray et al. 2005; Power et al. 2011) and numerically (e.g. Di Matteo et al. 2005; Booth & Schaye 2009). The AGN wind feedback model (King 2003, 2005, 2010; Zubovas & King 2012, and references therein) is particularly promising, as it explains not only the observed correlations, but also other observable properties of galactic winds (e.g. Pounds et al. 2003,?; Pounds & Vaughan 2011;

Tombesi et al. 2010,?) and outflows¹ (e.g. Rupke & Veilleux 2011; Sturm et al. 2011). In this picture, the wind and outflow shocks initially occur fairly close to the SMBH, and are efficiently Compton-cooled. The outflow retains only the ram pressure $\simeq L_{\text{Edd}}/c$ of the black hole wind and has kinetic energy lower by a factor $\sigma/c \sim 10^{-3}$. Only when the SMBH mass approaches the critical mass $M_\sigma \simeq 3.7 \times 10^8 M_\odot$ (see equation 7 below) do the shocks move further away. The resulting geometrical dilution of the quasar radiation field now makes Compton cooling inefficient. The shocks are no longer cooled, and the outflows become energy-driven.

In two recent papers (King et al. 2011; Zubovas & King 2012) we investigated the properties of large (kiloparsec)–scale outflows in galaxies. These must be energy-driven, i.e. the outflow kinetic energy rate $\dot{E}_{\text{out}} = \dot{M}_{\text{out}} v_{\text{out}}^2 / 2 \simeq$

¹ For clarity, we distinguish between the black hole *wind*, the gas coming directly from the accretion disc around the SMBH, and the *outflow*, the outward movement of swept-up interstellar gas from the host galaxy. These two components undergo respectively reverse and forward shocks on each side of the contact discontinuity separating them. See the Figure in Zubovas & King (2012) for more details

* E-mail: kastytis.zubovas@le.ac.uk

$0.05L_{\text{Edd}}$, where L_{Edd} is the Eddington luminosity of the driving quasar. We showed that energy-driven outflows are able to clear galaxies of gas, turning them into red-and-dead spheroids.

However, in these papers, we only briefly touched upon the question of how much the SMBH mass grows as it expels the outflow from the galaxy, and this remains uncertain. There are two discrepant claims: Power et al. (2011) used an energy argument to conclude that the SMBH only needs to grow its mass by $\sim 40\%$ to expel the surrounding gas past the virial radius, while in King et al. (2011) we found that an outburst duration of $\sim 10^8$ yr is required, which would lead to the SMBH mass growing by about an order of magnitude.

We return to this problem in this paper. We also consider the difference between evolved spiral and elliptical galaxies in more general terms, as well as the dependence of the outflow properties on the galaxy environment. We find only a small uncertainty in our results stemming from the assumption of an idealized background potential (Section 2). By considering the distribution of energy in various components of the outflow we resolve the discrepancy between the two claims (Section 3). We conclude that SMBHs in elliptical galaxies should grow to a mass a few times higher than in spirals for a given value of σ . We consider the effects of gas depletion and replenishment in a galaxy and find that galaxies in cluster environments should have slightly more massive SMBHs than their counterparts in the field (Section 4). We summarize and discuss our results in Section 5.

2 OUTFLOWS IN A GENERAL POTENTIAL

In previous work on the wind feedback model, we adopted an isothermal background potential, which has the useful property that the weight of the gas is independent of radius. To check the validity of this assumption we now consider what happens to an energy-driven (large-scale) flow in a more realistic halo. As an example we consider an NFW halo (Navarro et al. 1997). We note that McQuillin & McLaughlin (2012) have considered this problem assuming *momentum-driven* flows for all radii (also for Hernquist and Dehnen–McLaughlin potentials) and shown that the differences from the simple isothermal treatment are fairly small.

One particular difference between isothermal and NFW halos that is important for us is the varying velocity dispersion. In general, all non-isothermal halos have varying σ , usually with σ increasing from the centre out to some radius r_{peak} and decreasing beyond it. As the weight of the gas swept up by the outflow depends on the value of σ through the equation governing its density, it is no longer independent of radius, as is the case for an isothermal distribution. Specifically, the weight of the gas increases as the outflow moves from low radii toward r_{peak} and decreases afterwards. This means that an SMBH is able to inflate a rather large (but still with $R < R_{\text{peak}}$) outflow bubble even though its mass may still be too small to completely drive the gas out of a galaxy. On the other hand, once the outflow passes R_{peak} , it becomes easier to expel the gas.

In the present calculations, we consider an NFW halo with a concentration parameter (Navarro et al. 1997) $c =$

10, scale radius $R_s = 25$ kpc (so that $R_V = 250$ kpc) and virial mass $M_V = 3.3 \times 10^{12} M_\odot$. This gives $\sigma_{\text{peak}} \simeq 200$ km s^{-1} at $R_{\text{peak}} \simeq 2.16R_s \simeq 54$ kpc. We take the initial SMBH mass to be $M_0 = 3.68 \times 10^8 M_\odot$, equal to the critical SMBH mass found in previous papers (e.g. King 2010). We compare this NFW halo with an isothermal halo with $\sigma = 200$ km/s. We do not truncate either halo beyond R_V , but allow them to continue to infinity.

The equation of motion for an energy driven-shell in an isothermal potential was derived by King (2005) and its solutions investigated in King et al. (2011). Here we derive a generic equation of motion, valid for any spherically symmetric mass profile, provided that the gas density traces the background potential density, i.e. $M_g(R) = f_g M(R)$ for any R , where f_g is called the gas fraction. We start with equations (15) and (16) of King (2005):

$$f_g \frac{d}{dt} [M(R) \dot{R}] + \frac{Gf_g M^2(R)}{R^2} = 4\pi R^2 P \quad (1)$$

and

$$\frac{d}{dt} \left[\frac{4\pi R^3}{3} \times \frac{3}{2} P \right] = \frac{\eta}{2} L_{\text{Edd}} - P \frac{d}{dt} \left(\frac{4\pi R^3}{3} \right) - \frac{Gf_g M^2(R)}{R^2} \dot{R}. \quad (2)$$

Using eq. (1) to eliminate P from eq. (2) and expanding the terms with derivatives leads to a generalized equation of motion (we have dropped the (R) identifier from each mass for compactness):

$$\frac{\eta}{2f_g} L_{\text{Edd}} = \frac{3}{2} \frac{GM^2 \dot{R}}{R^2} + \frac{GM \dot{M}}{R} + \frac{3}{2} M \ddot{R} \dot{R} + \frac{3}{2} \dot{M} \dot{R}^2 + \frac{M \ddot{R} \dot{R}}{2} + \dot{M} \ddot{R} + \frac{\dot{M} \ddot{R} \dot{R}}{2}. \quad (3)$$

Here, $\dot{M} = \partial M / \partial R \times \dot{R}$ and $\ddot{M} = \partial M / \partial R \times \ddot{R} + \dot{R}^2 \times \partial^2 M / \partial R^2$. This equation reduces to eq. (18) of King (2005) in the case of an isothermal potential.

For an NFW potential the equation cannot be solved analytically, so we integrate it numerically. This also allows us to follow the growth of the central black hole mass (which slightly affects L_{Edd} on the left hand side of (3)). Figure 1 shows the propagation of four outflows, with $f_g = 3 \times 10^{-3}, 0.01, 0.03$ and 0.16 (lines from top to bottom in the top panel, respectively), in an isothermal potential (left) and an NFW potential described above (right). In both cases the SMBH is radiating and growing at the Eddington rate for $t = 90$ Myr = $2t_{\text{Sal}}$. Note that our results are valid only where the outflow velocity is $v_{\text{out}} < v_w \simeq 0.1c$. This condition is certainly satisfied when the gas density is high.

We see immediately that in an NFW halo, the outflows reach larger radii than in the isothermal case. This is expected, as the outflows are pushed past the radius of highest σ and so are able to accelerate to higher velocities before the central AGN switches off. The outflow velocity is almost constant during driving in the isothermal case, growing only in response to the growth of the SMBH ($v \propto M_{\text{BH}}^{1/3}$) and decays approximately as $v \propto t^{-1/2}$ afterwards. In the NFW case, the velocity is not constant, but the minimum velocity of the densest outflow is reached at $R \simeq R_{\text{peak}}$ and is similar to v_e , as might be expected.

From the results of the numerical integration it is clear that the isothermal potential probably represents a worst case scenario for outflow escape. In other words, the required AGN activity time and the final SMBH mass obtained using

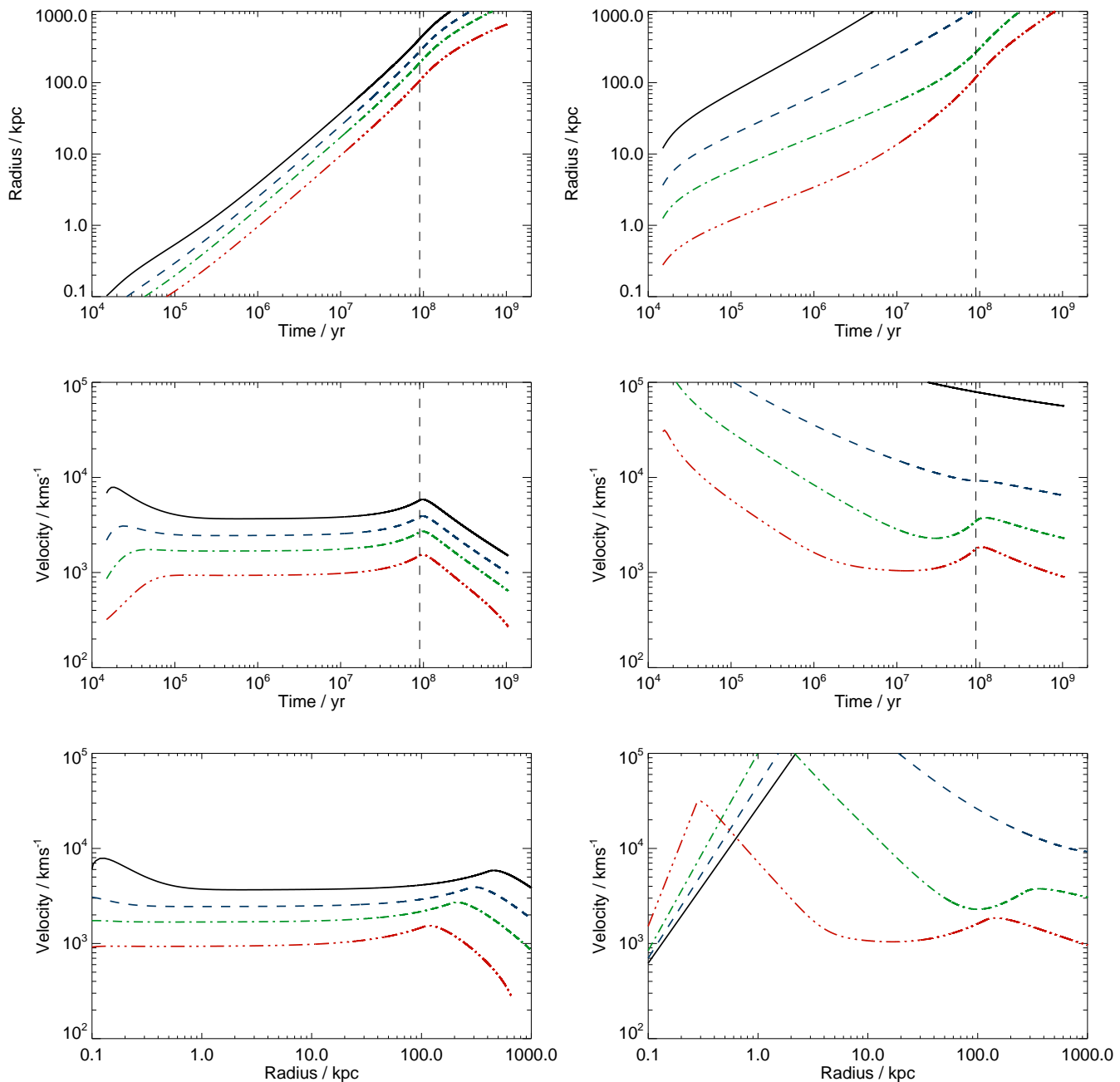


Figure 1. Propagation of energy-driven outflows in isothermal (left) and NFW (right) halos. The four outflows have $f_g = 3 \times 10^{-3}, 0.01, 0.03$ and 0.16 for the black solid, blue dashed, green double-dashed and red triple-dashed curves, respectively. The SMBH is active for 90 Myr (dashed vertical line in top and middle panels). As shown in King et al. (2011), outflow properties do not strongly depend on initial conditions (radius and velocity). *Top panels:* radius of the contact discontinuity as function of time. *Middle panels:* outflow velocity as function of time. *Bottom panels:* outflow velocity as function of radius.

the isothermal assumption are upper limits. This is reasonable, because the weight of the gas, which is $\propto \sigma^4$, is constant for the isothermal halo, whereas it varies and is always smaller for the NFW halo, which has $\sigma \leq \sigma_{\text{peak}} = \sigma_{\text{isotherm}}$.

The differences between the isothermal and NFW models are rather small for high gas density. For lower gas densities ($f_g \ll 0.16$), the outflow in an NFW potential reaches much higher velocities and escapes past R_V much faster.

However, since the higher density case is relevant for establishing the final SMBH mass (King 2003), we expect the uncertainty due to the shape of the background potential to be modest. This is reassuring in that earlier treatments of energy-driven outflows (e.g. King 2005; King et al. 2011) remain valid. However the question of the final SMBH mass remains. In the rest of this paper, we analyze this question in more detail. We use the singular isothermal sphere pro-

file of both gas and the background potential. We motivate our choice by the fact that analytical calculations are much more difficult, and often impossible, for non-isothermal potentials. In addition, using a different profile does not necessarily make our results more realistic: the central parts of galaxies, which are baryon dominated, are known to have profiles similar to isothermal (Naab et al. 2007), and even their dark matter profiles seem to differ from any known analytic profiles.

3 PROPERTIES OF LARGE SCALE OUTFLOWS

The radiation pressure of an active SMBH drives a quasi-spherical wind from the outskirts of its accretion disc (King 2010), which then hits and shocks against the ambient interstellar medium (ISM). The wind is mildly relativistic ($v_w \sim \eta c \sim 0.1c$, where η is the radiative accretion efficiency), and so its shock temperature is a few times 10^{11} K, much greater than the Compton equilibrium temperature ($T_C \sim 2 \times 10^7$ K). As we remarked above, the shocked wind therefore cools via the inverse Compton process against the photons of the AGN radiation field (Ciotti & Ostriker 1997). If the interaction between the wind and the ISM happens within a critical cooling radius (King 2003), the wind loses most of its original energy and only communicates its ram pressure to the ISM, creating a momentum-driven outflow (King 2010). Outside the cooling radius, on the other hand, the wind cannot cool efficiently and most of its energy rate $\dot{E}_w \simeq \eta L_{\text{Edd}}/2$ is communicated to the ISM, giving an energy-driven outflow (King 2005; Zubovas & King 2012).

3.1 Momentum-driven flows and $M - \sigma$ relation

We estimate the cooling radius R_C by comparing the wind cooling timescale (cf. King 2003):

$$t_C = \frac{2}{3} \frac{cR^2}{GM_{\text{BH}}} \left(\frac{m_e}{m_p} \right)^2 \left(\frac{c}{v_w} \right)^2 \simeq 10^7 R_{\text{kpc}}^2 M_8^{-1} \text{ yr}, \quad (4)$$

where M_8 is the SMBH mass M_{BH} in units of $10^8 M_\odot$, with the ISM flow timescale

$$t_{\text{flow}} \sim \frac{R}{v_{\text{out,m}}} \simeq 7 \times 10^6 R_{\text{kpc}} \sigma_{200} M_8^{-1/2} \left(\frac{f_g}{f_c} \right)^{-1/2} \text{ yr}, \quad (5)$$

where σ_{200} is the velocity dispersion in units of 200 km/s, $v_{\text{out,m}}$ is the *momentum-driven* outflow velocity (see equation (14) in King 2003), and $f_c = 0.16$ is the cosmological value of the baryon-to-dark-matter density fraction. Equating the two we find

$$\begin{aligned} R_C &\simeq \frac{3GM}{2c} \left(\frac{m_p}{m_e} \right)^2 \left(\frac{v_w}{c} \right)^2 \left(\frac{f_g \kappa \sigma^2}{2\pi G^2 M} \right)^{1/2} \\ &\sim 520 \sigma_{200} M_8^{1/2} v_{0.1}^2 \left(\frac{f_g}{f_c} \right)^{1/2} \text{ pc}. \end{aligned} \quad (6)$$

Here $v_{0.1}$ is the wind velocity in units of $0.1c$. If we had used an expression for the energy-driven outflow velocity (e.g. eq. 13 from King et al. 2011) rather than the momentum-driven one, the cooling radius would be smaller, so it is the momentum-driven velocity that is relevant here. We note that the value of R_C depends strongly on the assumed wind

velocity; while theoretically we expect it to always be similar to $0.1c$, observations (Tombesi et al. 2010,?; Pounds et al. 2003,?) suggest that it may vary from $\sim 0.03c$ to $\sim 0.2c$, leading to variations in R_C between ~ 50 pc and ~ 2 kpc for a $10^8 M_\odot$ black hole in a $\sigma = 200$ km s $^{-1}$ potential.

We see that close to the SMBH, outflows are momentum-driven. They only become energy-driven once the SMBH reaches some critical mass which allows a driven outflow formally to reach any radius (King 2005). This mass is

$$M_\sigma = \frac{f_g \kappa}{\pi G^2} \sigma^4 \simeq 3.7 \cdot 10^8 \frac{f_g}{f_c} \sigma_{200}^4 M_\odot. \quad (7)$$

This value is very close to the observed $M - \sigma$ relation (Ferrarese et al. 2006), provided that $f_g \simeq f_c$. Note that in King (2003), the expression for M_σ had an extra factor of $1/2$ in it, because that paper simply assumed an escape velocity $\sim \sigma$, rather than the full gravitational potential. King (2005) used a full isothermal potential, which gives the expression (7). In King et al. (2011), we mistakenly gave the incorrect numerical value for M_σ , although we used the correct analytical expression.

3.2 Clearing the bulge of a spiral galaxy

Once the black hole mass reaches this value, the outflow can propagate to large scales as the SMBH continues to grow. The timescale for the outflow to reach the cooling radius is $\sim t_{\text{flow}}$ (eq. 5), i.e. 2–3 Myr for the depleted bulge. Then the outflow becomes energy driven and rapidly attains a much higher constant velocity

$$v_e \simeq \left(\frac{2\eta f'_g \sigma^2 c}{3f_c} \right)^{1/3} \simeq 925 \sigma_{200}^{2/3} \left(\frac{f'_g}{f_c} \right)^{-1/3} \text{ km s}^{-1}, \quad (8)$$

where f'_g is the gas fraction in the bulge during the outflow, typically of the same order as f_c for young galaxies. This outflow sweeps the bulge in an additional time

$$t_{\text{out,e}} \simeq \frac{R_b - R_C}{v_e} \sim (R_{\text{b,kpc}} - 0.5) \text{ Myr}. \quad (9)$$

For typical bulge sizes of 1–2 kpc, this amounts to another ~ 1 Myr of SMBH activity. Gas expelled from the bulge does not necessarily escape the galaxy altogether, but it may settle on to the galaxy disc, which is not affected by the outflow directly (Nayakshin et al. 2012), as part of the galactic fountain (Bregman 1980).

Overall, this expulsion means that the SMBH must be active for ~ 5 Myr after it reaches the $M - \sigma$ mass (7), even when the outflow propagates in an isothermal potential; in an NFW potential, the outflow would propagate faster and so the bulge would be cleared sooner. Even accreting at the Eddington rate (this may be possible contemporaneously with an outflow due to the presence of a massive accretion disc around the SMBH, which cannot be lifted by its wind due to large weight; see Zubovas & Nayakshin 2012; Zubovas et al. 2011; Nayakshin & Power 2010), the SMBH only grows its mass by $\sim 10\%$ during this time. Therefore, the value M_σ (eq. 7) is likely to be the approximate upper limit to the mass of supermassive black holes in the bulges of spiral galaxies.

3.3 Elliptical galaxies and the transition to red-and-dead

Following a major merger, a galaxy changes from spiral to elliptical morphology. This means that the size of the spheroid grows from a bulge several kpc across, to the scale of the whole galaxy, which may have a radius of tens of kiloparsecs. Major mergers tend to cause bursts of star formation followed by a burst of quasar activity some ~ 300 Myr later (Sanders et al. 1988; Gao & Solomon 1999; Canalizo & Stockton 2001; Combes 2001). This quasar outburst is presumably what drives most of the remaining gas out of the galaxy (Zubovas & King 2012), transforming it into a red-and-dead elliptical. Noting that the virial radius $R_V \gg R_C$, we may calculate the duration of quasar activity necessary to eventually drive the gas outside the virial radius of the galaxy (cf. King et al. 2011). Unlike in the simpler case of a bulge (eq. 9), we have to consider the expansion of the outflow bubble even after the quasar has switched off. The result, in that case, is

$$t_q \sim \frac{\sigma R_V}{v_e^2} \simeq \frac{1}{7H} \left(\frac{\sigma}{v_e} \right)^2 \sim 9 \times 10^7 \sigma_{200}^{2/3} \left(\frac{f_g}{f_c} \right)^{2/3} \text{ yr} \simeq 2t_{\text{Sal}}, \quad (10)$$

where H is the Hubble parameter and $t_{\text{Sal}} = 45$ Myr is the Salpeter time. We also allow some variation of the gas density by including a dependence on f_g . If the galaxy is almost devoid of gas already, the black hole only needs to be active for a very short time to drive an outflow past R_V . This is also evident from the top panels of Figure 1. For a high gas density $f_g \sim f_c$, as may be expected after a major gas-rich merger, we see that the final mass of the black hole is

$$M_{\text{fin}} \sim M_\sigma \times \exp(2) \sim 7.5M_\sigma. \quad (11)$$

So the final mass of the SMBH in the centre of a red-and-dead elliptical galaxy is expected to be almost an order of magnitude greater than that inside a spiral galaxy with a red bulge exhibiting low star formation rate and low gas density.

This result disagrees with the estimate in Power et al. (2011), where we found, using an energy argument, that the SMBH only needs to grow for $\sim 0.4t_{\text{Sal}}$ in order to impart enough energy to the gas to let it escape past the virial radius. There are two complications with this calculation which give rise to the discrepancy. The first, minor, issue is that we used the formal escape velocity from an isothermal potential, $v_{\text{esc}} = 2\sigma$, to obtain the required energy input. However, the escape velocity is not well defined for an isothermal potential, and the adopted value 2σ only moves gas to a position with radius a factor 20 larger. As a result, gas initially within $R_V/20 \sim 20$ kpc needs more energy input to escape outside the virial radius. Nevertheless, this effect by itself only produces a small correction.

The second issue is more important. As an escape condition, we compare the virial radius of the galaxy with the radius of the contact discontinuity between the wind and the outflowing ISM. Even while the quasar is active and the outflow proceeds with velocity v_e , two-thirds of the input energy is transferred to the ISM *outside* the discontinuity (Zubovas & King 2012). After the quasar switches off, this fraction increases above $2/3$. By the time the outflow stalls, numerical simulations (Zubovas & Nayakshin 2012)

show that the energy content of the shocked wind is only a few percent of the total input energy. This happens because most of the shocked wind energy is thermal, and the wind cools as it expands, transferring energy to the outflow; by the time the outflow stalls, the energy per unit mass is roughly the same in both the wind and the ISM, so the ISM, which contains most of the mass, also has most of the energy.

All this means that in order to get the inner surface of the swept-up host ISM (the contact discontinuity) to expand past R_V , the quasar has to be active for at least a few times longer, and perhaps an order of magnitude longer, than estimated by Power et al. (2011). This correction brings the quasar duration required by energy arguments Power et al. (2011) into agreement with that required by the bubble dynamics, as here.

We can now combine the final SMBH mass derived above (eq. 11) and the bulge stellar mass estimate from Power et al. (2011),

$$M_b \lesssim 0.6\zeta M_{g,\text{vir}} \sigma_{200}, \quad (12)$$

where $\zeta \sim 1$ is a factor encompassing our uncertainty regarding the amount of feedback that self-regulated star formation produces when compared with the typical gas momentum in the bulge, and $M_{g,\text{vir}}$ is the total gas mass inside the virial radius of the galaxy. Together with the formulae for mass of an isothermal sphere and the virial radius (equations 3 & 18 in King et al. (2011), respectively), they give us the black hole - bulge mass relation:

$$\frac{M_{\text{fin}}}{M_b} \simeq 7.5 \times 3.7 \times 10^8 \sigma_{200}^4 \frac{7GH}{0.6\zeta \times 2f_c \sigma^3 \sigma_{200}} \sim 3 \times 10^{-3} \zeta^{-1}. \quad (13)$$

This is consistent with the observed relation (e.g. Häring & Rix 2004). For spiral galaxies, the black hole mass is approximately an order of magnitude lower, but the spheroidal component is also smaller by a similar factor, so the relation holds roughly in this case as well.

4 GALAXY ENVIRONMENT AND ITS INFLUENCE ON THE $M - \sigma$ RELATION

So far, in our calculations we have assumed that $f_g \simeq f_c$ throughout the evolution of a galaxy. This may be a reasonable assumption on scales larger than R_V , but is unlikely to be correct on the smaller scales that most immediately affect the properties of the black hole. Galaxy bulges are baryon-dominated and so by the time the SMBH begins driving large-scale outflows, the fraction of gas remaining in the bulge depends mainly on depletion by star formation and refilling via mergers or accretion of cold gas from the halo.

4.1 Gas depletion

When a galaxy forms, its central regions have $f_g \sim 1$, as most of the baryons have not yet had time to form stars. Subsequently, star formation depletes the gas on a timescale t_{SF} . As a rough approximation, we assume that star formation persists throughout the lifetime of the galaxy, with 2% of gas converted into stars on a dynamical time (Kennicutt

1998). With a scale radius for the bulge of 1 kpc, typical for a spiral galaxy, this gives a star formation timescale

$$t_{\text{SF}} = \frac{t_{\text{dyn}}}{\epsilon_{\text{SF}}} \simeq 2.5 \times 10^8 R_{\text{kpc}} \sigma_{200}^{-1} \epsilon_{0.02}^{-1} \text{ yr} \simeq 5.5 t_{\text{Sal}}. \quad (14)$$

If the SMBH grows from a seed mass of $\sim 10 M_{\odot}$, it takes $\sim 16 t_{\text{Sal}}$ to reach $10^8 M_{\odot}$, by which time the gas fraction is depleted to

$$f'_{\text{g}} \simeq \exp\left(-\frac{16 t_{\text{Sal}}}{t_{\text{SF}}}\right) \sim 0.05 \simeq 0.35 f_{\text{c}}. \quad (15)$$

Substituting f'_{g} instead of $f_{\text{g}} = f_{\text{c}}$ into equation 7 we find that in spiral galaxies we may expect SMBH masses to be a factor ~ 2.5 lower than predicted above.

The estimate above, however, is highly uncertain. At least three major effects may drive it to either higher or lower estimates for the SMBH mass. The estimate may be decreased if the SMBH growth is intermittent, i.e. the duty cycle is low, while star formation efficiency is approximately constant throughout the lifetime of the galaxy. In that case, the gas fraction in the bulge may be depleted to even lower values than f'_{g} , leading to a smaller critical SMBH mass. If, for example, the black hole duty cycle is 10% (Schawinski et al. 2007), then the critical black hole mass drops to a very low value of $10^4 M_{\odot}$. The fact that such small black holes are not observed suggests that star formation and SMBH growth are temporally correlated in galaxies.

On the other hand, there have been suggestions that SMBHs may grow from seeds as massive as $10^5 M_{\odot}$ (e.g. Begelman et al. 2006). In this case, the SMBH growth timescale is shorter than the $16 t_{\text{Sal}}$ used above, and so the gas is only depleted to $f_{\text{g}} \sim 0.4$, requiring a larger final SMBH mass.

Finally, a third complication may affect the slope of the predicted $M_{\text{BH}} - \sigma$ relation. Galaxies with larger σ have larger effective radii and larger bulges (e.g. Marconi & Hunt 2003) and so presumably are less efficient in forming stars. As a result, the critical value of f_{g} may correlate positively with σ , increasing the slope of the mass - velocity dispersion relation. This may be important when comparing spiral and elliptical galaxies: not only do elliptical galaxies need to grow their SMBHs for longer in order to expel the gas past the virial radius (see Section 3.3), they must do so while the galaxy has a higher gas fraction than a spiral galaxy would. However, we cannot quantify this effect in more detail without recourse to a much more detailed model of long-term galaxy evolution, which is beyond the scope of this paper.

A conclusion of this section is that it is likely, but by no means certain, that isolated spiral galaxies could have central SMBHs that are a factor ~ 2.5 less massive than predicted previously. Isolated elliptical galaxies may be similarly offset from the relation given in eq. (11). In addition, the slope in the $M - \sigma$ relation for these galaxies may be slightly steeper than $M \propto \sigma^4$ due to a correlation between the velocity dispersion and size of the galaxy spheroidal components.

4.2 Gas replenishment in clusters

The calculations above are valid for field galaxies, where internal processes of gas depletion dominate. If a galaxy falls

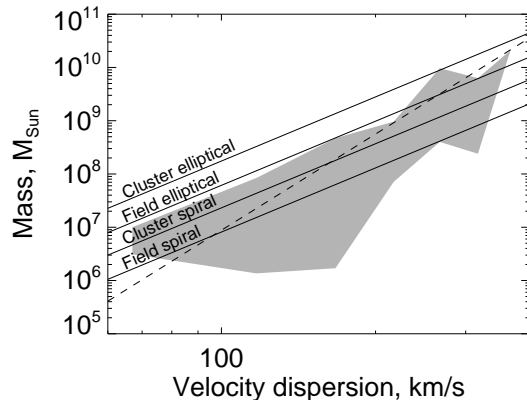


Figure 2. The four $M - \sigma$ relations (solid lines) and their combined effect on observational fits (dashed line). All solid lines have slopes $M \propto \sigma^4$ and the dashed line has $M \propto \sigma^6$. The grey area is the approximate locus of data points in Fig. 3 of McConnell et al. (2011).

inside a cluster, ram pressure and tidal forces strip most of its gas away (e.g. Takeda et al. 1984). This process lowers the average gas fraction in the galaxy; however, since gas is predominantly stripped from the outskirts of the galaxy (Abadi et al. 1999) and star formation is suppressed in line with gas depletion (Lewis et al. 2002; Balogh et al. 2000), the limiting central SMBH mass is not significantly affected by this process.

The cluster environment may also provide a replenishment of gas for galaxies that do not experience significant stripping, such as Brightest Cluster Galaxies (BCGs). These galaxies sit close to the centre of the cluster potential and thus are embedded in a massive hot halo. Cooling flows from the halo replenish gas in the galaxy (Fabian 1994), sustaining star formation and feeding the SMBH. If this replenishment happens on a timescale which is not too different from the cluster dynamical timescale $t_{\text{d,cl}} = R_{\text{cl}}/\sigma_{\text{cl}}$, then the two effects of star formation and cooling flow replenishment balance each other at a gas fraction

$$f_{\text{eq}} = \frac{t_{\text{SF}}}{t_{\text{d,cl}} + t_{\text{SF}}}. \quad (16)$$

Using the same values as above for star formation and $R_{\text{cl}} = 1$ Mpc and $\sigma_{\text{cl}} = 1000$ km/s, we find

$$f_{\text{eq}} = 0.2 \simeq f_{\text{c}}. \quad (17)$$

We see that BCGs, and perhaps some other cluster galaxies which are moving slowly with respect to the cluster halo gas, should have black hole masses governed by the M_{σ} of equations 11 and 7. The latter equation may apply to the strongly perturbed spiral galaxies which have lost most of their disc and so transformed to S0 morphological type, but still have only a small bulge which can be cleared easily and rapidly by the AGN.

5 DISCUSSION

We have shown that supermassive black holes residing in the bulges of spiral galaxies should have an $M - \sigma$ relation that

can be approximated by a power law slightly steeper than $M \propto \sigma^4$, if gas depletion due to star formation is considered. Typically, such galaxies would have $M < M_\sigma$ as predicted in our earlier papers (King 2003, 2010; King et al. 2011). During an event triggering strong central accretion, such as a major merger, the SMBH is likely to grow by a further factor of $\lesssim 7.5$ (i.e. for $\lesssim 2$ Salpeter times) before it can drive the gas out of the galaxy halo. This factor is an upper limit, because we calculated it for an isothermal background potential, which is the most difficult to escape from.

One might think that since the SMBH is not immediately aware of the processes occurring around the virial radius of the halo, it could grow for longer than the calculated ~ 2 Salpeter times, as long as the gas reservoir feeding it is not depleted. However, the total mass of gas that must be accreted in this process is of order $10^9 M_\odot$, perhaps even more. This is too high to reside in a single accretion disc, and the SMBH is very probably fed in a series of stochastic feeding events (King & Pringle 2007; Nayakshin & King 2007). Feedback therefore affects the SMBH feeding reservoir, and so it seems more likely that the reservoir is fairly efficiently depleted. While gas may fall back on to the SMBH if it has not yet escaped the halo and trigger subsequent bursts of activity, it cannot do so once the halo is depleted, so the AGN should switch off very soon after the outflow clears the galaxy.

Our results suggest that there should be a difference between the $M - \sigma$ relations for spiral star-forming galaxies and for red and dead ellipticals. The latter should have SMBHs that are systematically overmassive when compared with the prediction of the $M - \sigma$ relation for the spiral galaxies. This mass difference is not huge - less than an order of magnitude - but it may become apparent when better SMBH mass and spheroid velocity dispersion measurements become available.

There is another possible offset in the $M - \sigma$ relation depending on the galaxy environment. Galaxies in clusters, especially those residing near cluster centres, may accrete gas from the hot cluster halo via cooling flows. This process may balance the depletion by star formation at a gas fraction ~ 0.2 , preserving the old $M - \sigma$ relationship (eq. 7) in galaxies that had been spirals by the time they entered the cluster environment; even though they lose most of the gas from the outskirts, the central spheroidal component remains unperturbed and the analysis in Section 3.2 still applies. Cluster ellipticals would also be a factor $\lesssim 7.5$ more massive. On average, cluster galaxies have black holes slightly more massive (by a factor ~ 2.5) than their field counterparts. Our findings are consistent with the recent discovery of two SMBHs in the centres of giant elliptical galaxies that have masses in excess of $10^{10} M_\odot$. They are both Brightest Cluster Galaxies and our model predicts that their masses should be approximately an order of magnitude above the relation derived in earlier works.

In summary, we have found that there may be three (or possibly even four) $M - \sigma$ relations in total, depending on galaxy morphology and environment:

- spiral galaxies with evolved bulges have $M_{\text{BH}} \sim 1.3 \times 10^8 \sigma_{200}^{4+\beta} M_\odot$ with $\beta \lesssim 1$ depending on star formation efficiency and the relation between the bulge size and σ ;
- spiral galaxies with evolved bulges residing in gas-rich

cluster environments have $M_{\text{BH}} \sim 3.7 \times 10^8 \sigma_{200}^4 M_\odot$ (the original $M - \sigma$ relation); such galaxies, however, may be extremely rare due to high merger probability in clusters;

- field elliptical galaxies have $M_{\text{BH}} \sim 9.8 \times 10^8 \sigma_{200}^{4+\zeta} M_\odot$;
- elliptical galaxies close to cluster centres have $M_{\text{BH}} \sim 28 \times 10^8 \sigma_{200}^4 M_\odot$.

There is some uncertainty in the slope, especially for field galaxies. It is clear that, as bigger bulges have larger velocity dispersions, the slope should be steeper than 4, but its precise value depends strongly on the assumed relation between R_b and σ (both its slope and intercept).

The differences among the four relations are small, at most factors of a few in the normalization. Intrinsic scatter in each population may blur the distinctions further. In addition, since elliptical galaxies tend to have higher velocity dispersions than spirals, and cluster galaxies than field galaxies, the overall effect of combining the relations may be to increase the observed slope of the $M - \sigma$ relation. We illustrate this in Figure 2. We plot the four $M - \sigma$ relations (assuming $\beta = 0$) over a polygon representing the approximate locus of data points taken from Figure 3 of McConnell et al. (2011). All four lines intersect the locus. The large fraction of the locus being below the four lines is reasonable since the predicted relations are only upper limits for different environments. Furthermore, there is a hint that higher values of σ correspond to higher $M - \sigma$ relations. We also plot a line with $M \propto \sigma^6$, which roughly bisects the observed locus and so might emerge from a fit to the data unsorted by galaxy type, especially in the $\sigma > 100$ km/s part, where we do not expect contamination from nuclear stellar clusters (McLaughlin et al. 2006; Ferrarese et al. 2006).

There have been recent tentative claims that the $M - \sigma$ relation may be slightly different for different galaxy types, and that the general relation may show an upturn at higher values of σ (Marconi & Hunt 2003; McConnell et al. 2011). Our considerations here suggest that both features may be natural consequences of wind feedback.

ACKNOWLEDGMENTS

We thank the referee for very detailed and thorough comments which allowed us to significantly improve the clarity of the paper.

Research in theoretical astrophysics at Leicester is supported by an STFC Rolling Grant. KZ is supported by an STFC research studentship.

REFERENCES

- Abadi M. G., Moore B., Bower R. G., 1999, MNRAS, 308, 947
 Balogh M. L., Navarro J. F., Morris S. L., 2000, ApJ, 540, 113
 Begelman M. C., Volonteri M., Rees M. J., 2006, MNRAS, 370, 289
 Booth C. M., Schaye J., 2009, MNRAS, 398, 53
 Bregman J. N., 1980, ApJ, 236, 577
 Canalizo G., Stockton A., 2001, ApJ, 555, 719
 Ciotti L., Ostriker J. P., 1997, ApJ, 487, L105+
 Combes F., 2001, in I. Aretxaga, D. Kunth, & R. Mújica ed., Advanced Lectures on the Starburst-AGN Fueling the AGN. p. 223
 Di Matteo T., Springel V., Hernquist L., 2005, Nature, 433, 604

- Fabian A. C., 1994, *ARA&A*, 32, 277
- Ferrarese L., Côté P., Dalla Bontà E., Peng E. W., Merritt D., Jordán A., Blakeslee J. P., Hasegan M., Mei S., Piatek S., Tonry J. L., West M. J., 2006, *ApJ*, 644, L21
- Gao Y., Solomon P. M., 1999, *ApJ*, 512, L99
- Häring N., Rix H.-W., 2004, *ApJ*, 604, L89
- Kennicutt Jr. R. C., 1998, *ApJ*, 498, 541
- King A., 2003, *ApJ*, 596, L27
- King A., 2005, *ApJ*, 635, L121
- King A. R., 2010, *MNRAS*, 402, 1516
- King A. R., Pringle J. E., 2007, *MNRAS*, 377, L25
- King A. R., Zubovas K., Power C., 2011, *MNRAS*, pp L263+
- Lewis I., Balogh M., De Propriis R., Couch W., Bower R., Offer A., Bland-Hawthorn J., Baldry I. K., Baugh C., Bridges T., Cannon R., Cole S., Colless M., Collins C., Cross N., Dalton G., Driver S. P., Efstathiou G., et al. 2002, *MNRAS*, 334, 673
- Marconi A., Hunt L. K., 2003, *ApJ*, 589, L21
- McConnell N. J., Ma C.-P., Gebhardt K., Wright S. A., Murphy J. D., Lauer T. R., Graham J. R., Richstone D. O., 2011, *Nature*, 480, 215
- McLaughlin D. E., King A. R., Nayakshin S., 2006, *ApJ*, 650, L37
- McQuillin R. C., McLaughlin D. E., 2012, *ArXiv e-prints*
- Murray N., Quataert E., Thompson T. A., 2005, *ApJ*, 618, 569
- Naab T., Johansson P. H., Ostriker J. P., Efstathiou G., 2007, *ApJ*, 658, 710
- Navarro J. F., Frenk C. S., White S. D. M., 1997, *ApJ*, 490, 493
- Nayakshin S., King A., 2007, *ArXiv e-prints*
- Nayakshin S., Power C., 2010, *MNRAS*, 402, 789
- Nayakshin S., Power C., King A. R., 2012, *ArXiv e-prints*
- Pounds K. A., King A. R., Page K. L., O'Brien P. T., 2003, *MNRAS*, 346, 1025
- Pounds K. A., Reeves J. N., King A. R., Page K. L., O'Brien P. T., Turner M. J. L., 2003, *MNRAS*, 345, 705
- Pounds K. A., Vaughan S., 2011, *MNRAS*, 413, 1251
- Power C., Zubovas K., Nayakshin S., King A. R., 2011, *MNRAS*, 413, L110
- Rupke D. S. N., Veilleux S., 2011, *ApJ*, 729, L27+
- Sanders D. B., Soifer B. T., Elias J. H., Madore B. F., Matthews K., Neugebauer G., Scoville N. Z., 1988, *ApJ*, 325, 74
- Schawinski K., Thomas D., Sarzi M., Maraston C., Kaviraj S., Joo S.-J., Yi S. K., Silk J., 2007, *MNRAS*, 382, 1415
- Silk J., Rees M. J., 1998, *A&A*, 331, L1
- Sturm E., González-Alfonso E., Veilleux S., Fischer J., Graciá-Carpio J., Hailey-Dunsheath S., Contursi A., Poglitsch A., et al. 2011, *ApJ*, 733, L16+
- Takeda H., Nulsen P. E. J., Fabian A. C., 1984, *MNRAS*, 208, 261
- Tombesi F., Cappi M., Reeves J. N., Palumbo G. G. C., Yaqoob T., Braitto V., Dadina M., 2010, *A&A*, 521, A57+
- Tombesi F., Sambruna R. M., Reeves J. N., Braitto V., Ballo L., Gofford J., Cappi M., Mushotzky R. F., 2010, *ApJ*, 719, 700
- Zubovas K., King A., 2012, *ApJ*, 745, L34
- Zubovas K., King A. R., Nayakshin S., 2011, *MNRAS*, 415, L21
- Zubovas K., Nayakshin S., 2012, *ArXiv e-prints*